CARBON 62 (2013) 322–329

Available at www.sciencedirect.com

SciVerse ScienceDirect

journal homepage: www.elsevier.com/locate/carbon

Rapid synthesis of foam-like mesoporous carbon monolith using an ultrasound-assisted air bubbling strategy

De-Cai Guo, Wen-Cui Li, Wei Dong, Guang-Ping Hao, Yuan-Yuan Xu, An-Hui Lu *

State Key Laboratory of Fine Chemicals, School of Chemical Engineering, Dalian University of Technology, Dalian 116024, PR China

ARTICLE INFO

Article history:
Received 5 April 2013
Accepted 4 June 2013
Available online 13 June 2013

ABSTRACT

Highly uniform foam-like carbon monolith with mesoporous structure has been synthesized using an ultrasound-assisted air bubbling strategy in self-assembled F127 and poly-(benzoxazine-co-resol)-based aqueous emulsions. The air bubbling strategy is easy and green as the use of additional inorganic foaming agent or solid templates is not required. Furthermore, it has been found that an ultrasound treatment initiates the rearrangement of surfactant F127 and induces the generation of a defective mesostructure. The synthesized foam-like carbon monolith has been evaluated as an electrode material for supercapacitors.

1. Introduction

Mesoporous carbon monoliths have advantages over their powder counterparts in the diverse fields of adsorption, separation, catalysis, micro-reactor, energy storage and conversion [1–5], due to for example, their low pressure drop and efficient heat and mass transfer. Many applications would benefit from the incorporation of macropores and uniform mesopores in the monolithic structure, allowing an easy access for guest molecules. Especially for the application of electrode material for supercapacitors, the continuous hierarchical porous structure provides an accessible passway for the electrolyte fast transportation in the carbon framework [6–9]. So it is desirable to explore a synthesis method to tune the carbon porosity with a continuous porous framework. To date, most reported methods rely on the self-assembly process of surfactants with carbon precursors [10–12], predominantly under hydrothermal conditions [10,13,14]. Alternatively, many macroporous carbon or foam-like carbon is prepared by using inorganic foaming agent or solid templates [15,16]. These disclosed methods allow precise control of pore sizes and structures [9,11,17]. However, there is still a requirement to develop a simple and scalable synthesis strategy for the preparation of hierarchical carbon monoliths with intrinsic macropores and mesopores.

It is well known that the ultrasound is a common tool used to synthesize inorganic materials [18,19], whereby the energy of sound waves are transferred to the reaction system and consequently generate bubbles. Using this principle, we report a simple and rapid synthesis route of an ultrasound-assisted air bubbling method for the fabrication of carbon monoliths with foam-like macropore system and mesopore structure. The synthesis involves ultrasound assisted bubbling air through a poly-(benzoxazine-co-resol)-based solution to form air stabilized emulsions, followed by a fast polymerization step at 90 °C. As a result, a homogeneous organic monolith is obtained, which can be converted to a foam-like mesoporous carbon monolith after carbonization. Compared to conventional methods [20] of preparing

* *Corresponding author:* Fax: +86 411 84986112.
E-mail address: anhuilu@dlut.edu.cn (A.-H. Lu).
0008-6223/$ - see front matter
http://dx.doi.org/10.1016/j.carbon.2013.06.015

foam-like carbons, the present method is simpler and greener in terms of time-saving, and being free of inorganic foaming agent and solid templates [21,22].

2. Experimental

2.1. Chemicals

Resorcinol (denoted R, 99.5%) and formaldehyde (37 wt%) were purchased from Tianjin Kermel Chemical Reagent Co., Ltd. 1,6-Diaminohexane (DAH, 99.0%), ethanol (99.7%), were all supplied by Sinopharm Chemical Reagent Co., Ltd. Pluronic F127 was purchased from Sigma–Aldrich. All chemicals were used as received.

2.2. Synthesis of the foam-like carbon monolith

In a typical synthesis, 0.5 g of resorcinol and 0.301 g of Pluronic F127 were dissolved in a 3 g solvent mixture of ethanol and deionized water (1:1 wt%) with magnetic stirring at 25 °C. Then 0.026 g 1,6-diaminohexane was added into the above solution and stirred for *ca.* 5 min at 25 °C. Subsequently, 0.735 g of formaldehyde solution (denoted F) was quickly injected into the solution to form a white homogeneous emulsion over a very short period (<1 min). Then air was bubbled through the emulsion using a capillary glass tube. Simultaneously the vessel was dipped into an ultrasound bath of 90 °C and ultrasound treatment with a power of 100 W and frequency of 80 kHz was used during the bubbling process. After 20 min, a white homogeneous emulsion formed that was full of foam, and the color gradually turned from white to light jacinth. After switching off the air bubbling, the jacinth foam polymer was isolated and transferred to a box oven at 90 °C for 4 h curing. Subsequently, the as-made polymer monolith was dried at 50 °C in air for 24 h, and then carbonized at 800 °C under a nitrogen atmosphere for 2 h to obtain a crack-free foam-like carbon monolith (denoted FMCM-U). Furthermore, to highlight the role of the ultrasound treatment in the bubbling process, another foam-like carbon monolith (denoted FMCM) was synthesized in the absence of ultrasound treatment to be used as a control. The amounts of DAH and F127 were also varied, respectively and the detailed synthesis conditions were listed in Table 1. The samples were denoted as FMCM-U-1 and FMCM-1. The determined yields of all carbon samples are quite similar and approximately 35%.

2.3. Characterization

Scanning electron microscope (SEM) investigations were carried out with a Hitachi S-4800I instrument at 10 kV. Transmission electron microscopy (TEM) images of the samples were obtained with a Tecnai G20S-Twin electron microscope equipped with a cold field emission gun. The acceleration voltage was 200 kV. Samples were prepared by dropping a few drops of a suspension of one sample in ethanol onto the holey carbon grid with a pipette. Nitrogen adsorption isotherms were measured with an ASAP 2020 sorption analyzer (Micromeritics). The Brunauer-Emmett-Teller (BET) method was utilized to calculate the specific surface areas (S_{BET}). Pore size distributions (PSDs) were determined from the desorption branches of the isotherms using the Barrett-Joyner-Halenda (BJH) model. Total pore volumes (V_{total}) were calculated from the amount adsorbed at a relative pressure (P/P_0) of 0.99. Micropore volumes (V_{micro}) were calculated using the t-plot method. The X-ray diffraction (XRD) measurements were taken on a Rigaku D/Max 2400 diffractometer using CuK_α radiation (40 kV, 100 mA, $\lambda = 1.5406$ Å). The compressive strength is the maximum stress supported by the samples during the test, i.e., the stress at which macroscopic failure occurs. Tests were performed at a strain rate of 1 mm min^{-1}. All measurements were recorded at *ca.* 25 °C and 70% relative humidity. Samples were of cylinder shape, carefully machined to ensure perfectly parallel bases and a length/diameter ratio of 1.

2.4. Electrochemical measurements

The working electrodes were prepared by mixing 80 wt% porous carbons as the active materials, 10 wt% conductive carbon black and 10 wt% polytetrafluoroethylene (PTFE) in 7 mL ethanol. The slurry of the mixture was rolled into a film, cut into suitable shapes and placed into an oven at 150 °C for 4 h. The films were then put onto a nickel foam current collector with area of 1 cm^2 and pressed under a pressure of 10 MPa for 5 min to fabricate the electrode. The mass loading of the active material was between 4 and 6 mg cm^{-2}. The capacitive performance of the single electrode was carried out on an CHI660D electrochemical workstation (CH Instruments Inc., Shanghai, China) using a standard three-electrode test system composed of Hg/HgO as the reference electrode and Pt plate as the counter electrode in 6 M KOH electrolyte at 25 °C. Cyclic voltammetry (CV), electrochemical impedance

Table 1 – Synthesis conditions, texture parameters and elemental compositions of the foam-like carbon monolith.

Sample	Molar ratio of R /F127/amine	Ultrasound assistant*	Texture parameters				Elemental analysis, wt.%			
			S_{BET} (m^2 g^{-1})	D_{peak} (nm)	V_{total} (cm^3 g^{-1})	V_{mic} (cm^3 g^{-1})	C	N	H	O
FMCM	275:1.44:13.6	N	626	4.8	0.42	0.20	87.97	0.41	1.83	9.79
FMCM-U	275:1.44:13.6	Y	678	5.9	0.50	0.21	88.10	0.37	1.67	9.86
FMCM-1	275:1.44:27.2	N	645	4.0	0.35	0.23	87.55	0.70	1.96	9.79
FMCM-U-1	275:1:13.6	Y	585	5.7	0.35	0.20	89.01	0.36	1.80	8.83

* N stands for without the assistant of ultrasound and Y stands for with the assistant of ultrasound during the synthesis process.

and galvanostatic charge–discharge (GC) measurements were employed in the evaluation of the electrode electrochemical performance. The specific capacitance of the materials were calculated using the equation $C(F\ g^{-1}) = \frac{I\Delta t}{m\Delta V}$, where I (A), Δt (s), ΔV (V) and m (g) are the discharge current, the discharge time, the operation potential window from the end of the voltage drop to the end of the discharge process and the mass of active materials, respectively [23].

3. Results and discussion

The synthesis procedure is schematically illustrated in Fig. 1a, and the corresponding photographs of air bubbling, foam-like polymer and carbon monoliths are shown in Fig. 1b. The route developed in the current study consists of the following principal steps. In the first step, the emulsion constituted by a stable oligomer of poly-benzoxazine segments is formulated by the Mannich reaction. Next, during the bubbling air process, at the interphase of solid (oligomer), liquid (alcohol/water solution) and gas (air), surfactants assemble into a micelle structure that keep the hydrophilic parts of the surfactant in contact with solution while shielding the hydrophobic parts within the micellar interior. In the meantime, the foamed emulsion particles stabilize the air bubble, which is not only stabilized by the rapidly generated polymer building-blocks through a decrease of the gas–liquid interfacial tension but also following the evaporation of the solution. Benefiting from a fast gelation (which causes a high viscosity of the emulsion, during the following curing step), a fully polymerized porous poly-(benzoxazine-co-resol) is obtained. After carbonization, a foam-like carbon monolith with macrocellular structure and mesopores is achieved.

Conventionally, the generation of polymeric foams depends on the complex interplay between the initial foaming ability and the subsequent drainage, which themselves are related to the surface and bulk rheological properties. It is known that the foam instability arises from the high energy associated with the gas–liquid interphase, and constitutes a driving force for decreasing the total interfacial area of the foam through coalescence and disproportionation of the bubbles. Minimizing the drainage speed is a critical factor in preventing the coalescence of foams, so the rapid solidification of the foam framework is a crucial element for the synthesis of stable foams. Previous research has shown that a benzoxazine-co-resol system can be rapidly polymerized in a few minutes [24]. Taking advantage of the fast solidification of the poly-(benzoxazine-co-resol) oligomer emulsion, we could obtain air bubbled polymer foams under mild reaction conditions: at 1 atm and 90 °C, and a short reaction time of 20 min. As a result, a foam-like carbon monolith with macrocelluar structure and mesopores can be obtained (Fig. 1b).

Fig. 1b displays a typical image of the foamed polymer monolith and the corresponding carbon product. Both present a homogeneous foam cell distribution. Further observations reveal the presence of networks with well-defined interconnected large macropores with diameters in the range of several hundreds of microns. The densities of the synthesized polymer and carbon monolith are estimated to be

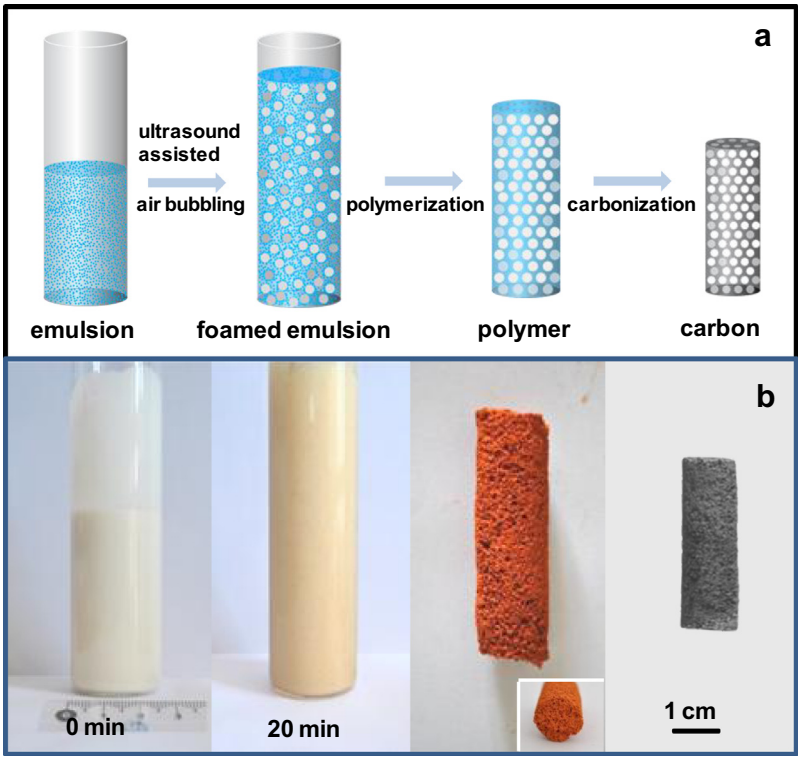

Fig. 1 – Illustration of the preparation for foam-like mesoporous carbon monolith through the ultrasound-assisted air bubbling strategy (a), and the photographs of the obtained foam-like polymer and the corresponding carbon monoliths (b).

0.103 g cm^{-3} and 0.092 g cm^{-3}, respectively. By choosing different reaction vessels, we can in principle tune the dimensions and sizes of the foam-like carbon monoliths.

The SEM images (Fig. 2a and b) further verify a continuous framework and open structure with interconnected pores between the cells. When using the air bubbling method, foam-like carbon FMCM with a broad macropore size distribution ranging from 100 to 300 μm can be prepared. While, with the aid of the ultrasound in the air bubbling process, the obtained sample FMCM-U shows a greater degree of macropore uniformity with the sizes concentrated around 200 μm. The thicknesses of the macropore walls range from 40 to 88 μm. Specifically, the interconnected foam skeleton walls are constituted by many secondary carbon particles (inset in Fig. 2a and b), which is a significant difference from the previously synthesized carbon foams [25–27].

During the foaming process, the copolymer family of surfactants can effectively suppress bubbles disappearance. Furthermore, it is known that when a sound wave travels through a liquid, natural occurring bubbles grow in size [28]. This affects the surfactant assembly and changes the morphology of the carbon framework. At the nanometer scale, the porous structures of the foam-like carbon monoliths FMCM and FMCM-U were analyzed by TEM. As shown in Fig. 2c, one can observe that sample FMCM prepared only with the air bubbling method generally shows worm-like mesopores. In contrast, sample FMCM-U prepared using the combination of air bubbling and ultrasound treatment, exhibits defective mesostructure [10,29,30] (Fig. 2d). The thickness of the mesoporous pore wall is estimated as *ca.* 6.9 nm. The center-to-center distances of adjacent channels are *ca.* 10.4 nm, and the porous diameter is *ca.* 6.0 nm. The detailed pore structure changes can be further verified from nitrogen adsorption isotherms measured at 77 K. As shown in Fig. 2e, the isotherms of FMCM and FMCM-U are type-IV in shape with a sharp uptake due to the capillary condensation effect, indicating a mesoporous feature. Ultrasound treatment results in an increase of the specific surface area from 626 to 678 m^2 g^{-1} and the total pore volume from 0.42 to 0.50 cm^3 g^{-1} (Table 1). Meanwhile, the mesopore sizes were enlarged from 4.8 to 5.9 nm (inset in Fig. 2e). Hence, the pore sizes determined from N_2 adsorption isotherms agree well with those derived from TEM measurements. The local mesostructure of FMCM-U can also be verified by the low-angle XRD pattern (Fig. 2f), which presents a weak and broad peak, corresponding to the short-range order of a mesostructure. On the contrary, there is no observed reflection in the XRD pattern of FMCM, indicating a worm-like pore arrangement.

To evaluate the mechanical strength of the foam-like mesoporous carbon monolith, the compressive strength, the

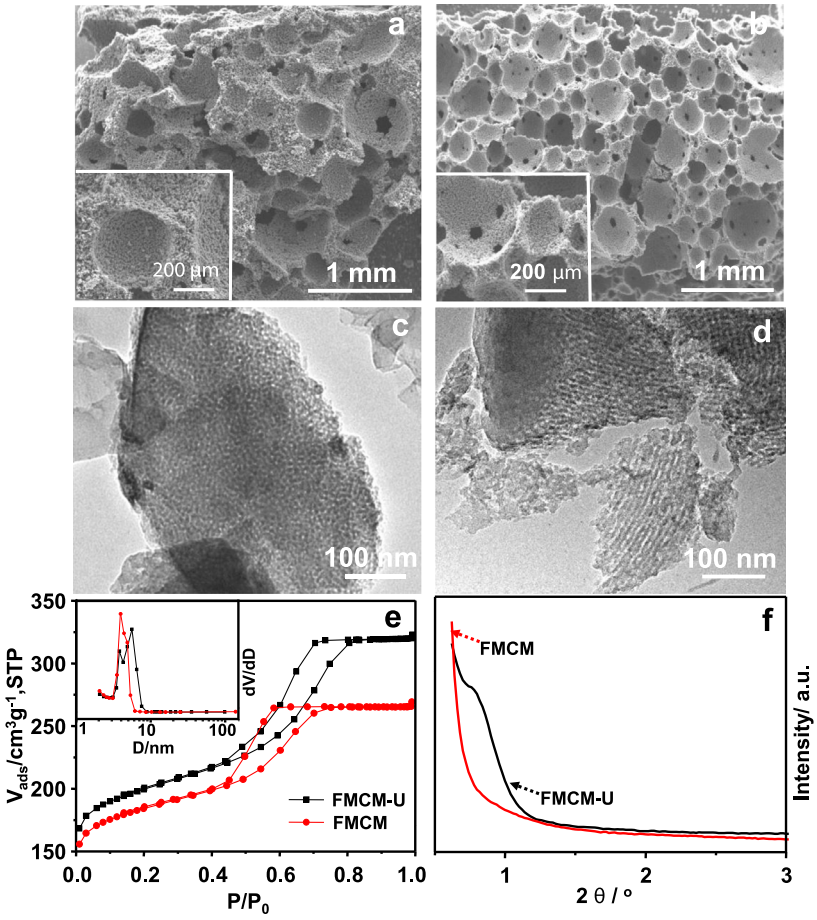

Fig. 2 – SEM images of FMCM (a) and FMCM-U (b), TEM images of FMCM (c) and FMCM-U (d), N_2 sorption isotherms of FMCM and FMCM-U (inset is the corresponding PSDs) (e), low-angle powder XRD patterns of FMCM and FMCM-U (f).

compressive force per unit area that a material can withstand, was measured. The FMCM-U and FMCM can respectively bear a load of 90.7 psi (0.62 MPa) and 58.1 psi (0.40 MPa), higher than those of the reported nanocasting carbon monolith (27.9 psi, 0.19 MPa) [11] and the soft-templated carbon monolith (29.3 psi, 0.2 MPa) [10]. Evidently, our newly developed foam-like carbon monolith possesses several salient features such as the fully interconnected macropores and mesopores and a certain degree of mechanical strength, and can be facilely prepared in a time-saving manner. Especially, the ultrasound assistant modulates and rearranges the surfactant F127, and then generates the mesostructure in carbon framework.

In order to demonstrate the reproducibility of this proposed air bubbling strategy, the amounts of DAH and F127 were varied and the obtained carbon monolith were named as FMCM-U-1 and FMCM-1. From the SEM images of FMCM-U-1 and FMCM-1, it further verifies the homogeneous foam cell distribution, the continuous framework and open structure with interconnected pores between the cells (Fig. 3a and b). The skeleton walls are also constituted by many secondary carbon particles. The N_2 sorption isotherms also present a typical type-IV shape, indicating a mesoporous feature (Fig. 3c). And the mesopore sizes are 5.7 and 4.0 nm for FMCM-U-1 and FMCM-1, respectively (Fig. 3d). So the ultrasound-assisted air bubbling strategy is an effective and reproducible method for synthesis of the foam-like carbon monolith in this reaction system. The elemental compositions of the samples are listed in the Table 1. It's clear that all of them contained a little amount of N, which is generated from the pyrolysis of DAH. The heteroatom contained carbon matrix has been confirmed helpful for the enhancement of the surface wettability and modulate the electronic properties of the carbon as well as producing additional functional groups on the carbon surface, resulting in an enhancement in the electrochemical performance [31–33].

A possible mechanism of the structure evolution by air bubbling combined with ultrasound treatment is proposed based on the above discussion: the air bubbling is a driving force to create a liquid and air interface, further increase the body concentration of the reaction system, and thus induce an arrangement of the surfactants [34–36]. Simultaneously, ultrasound treatment leads to more homogeneous emulsion foams, which drives the self-assembly of the oligomer-surfactant micelles into organized liquid mesophases. Thus, the combination of air bubbling and ultrasonic wave treatment promotes the self-organization of the surfactant micelles resulting in a more mesostructure foam-like polymer monolith, and consequently carbon monolith following pyrolysis.

Furthermore, the prepared foam-like carbon monoliths with a high surface area and a conducting mesoporous carbon skeleton were investigated as electrode material for supercapacitor, based on the principle that a large pore size can facilitate the access and rapid diffusion of electrolyte. The CV curves of FMCM and FMCM-U at a low scan rate of 5 mV s^{-1} (Fig. 4a and b) showed rectangular shapes, suggesting a typical double-layer capacitance behavior. When the scan rate was increased from 5 to 200 mV s^{-1}, a similar rectangular shape was mainly retained, indicating a good capacitive performance at high scan rates. The galvanostatic charge–discharge tests of the foam-like carbons were conducted at current densities from 0.5 to 10 A g^{-1}. As seen in Fig. 4c and d, the GC curves at different current densities showed isosceles triangular shapes, suggesting excellent coulombic efficiency and ideal capacitor behavior. Even at a high current density of 10 A g^{-1}, no sudden potential drop was observed, revealing that the electrochemical device made from the foam-like mesoporous carbon has low equivalent series resistance (ESR). The specific capacitances were calculated from the GC curves to be ~151 F g^{-1} for FMCM-U and

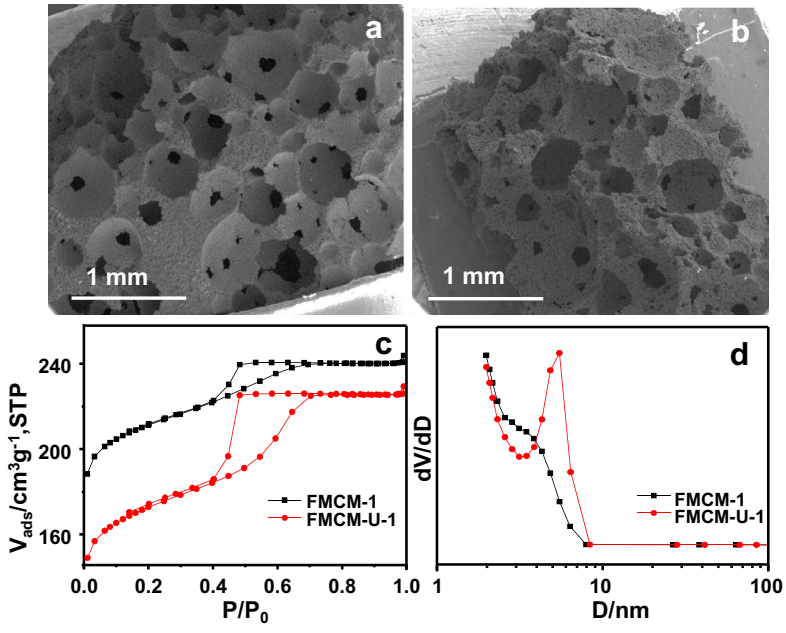

Fig. 3 – SEM imagines of FMCM-U-1 (a) and FMCM-1 (b); N_2 sorption isotherms of FMCM-1 and FMCM-U-1 (c) and the corresponding PSDs (d). The isotherm of FMCM-1 is offset vertically by 20 cm^3 g^{-1} STP.

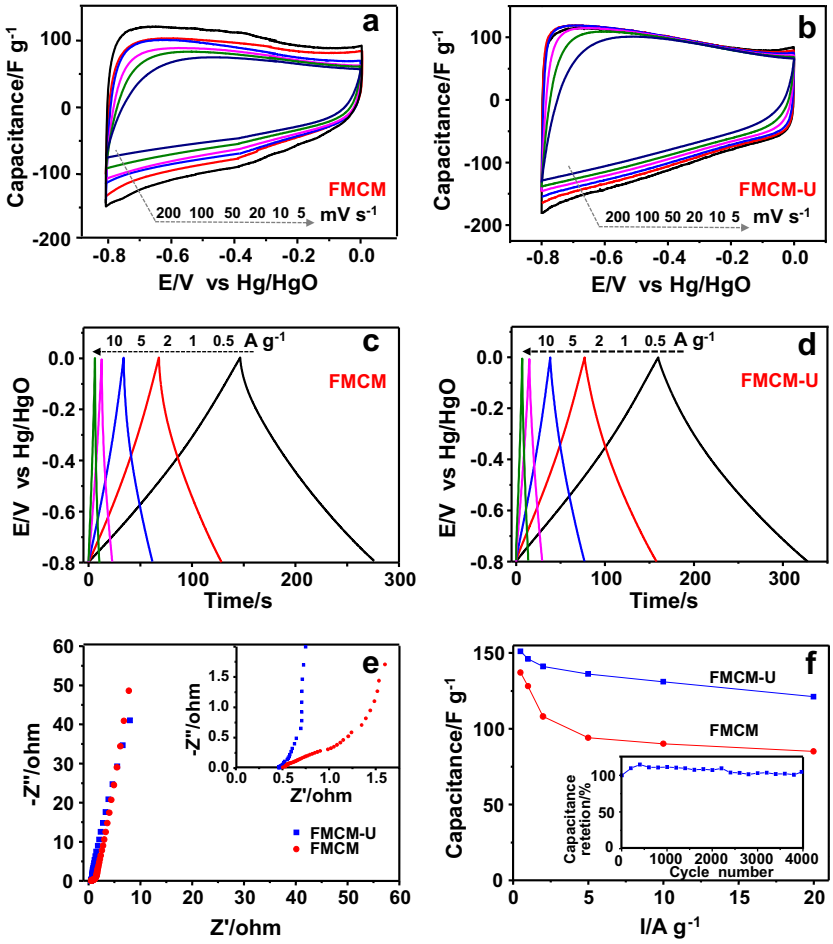

Fig. 4 – Cyclic voltammograms at various scan rates of FMCM (a) and FMCM-U (b). Charge–discharge curves at different current densities of FMCM (c) and FMCM-U (d). Nyquist plots in the frequency range of 100 kHz–10 mHz in KOH electrolyte at 25 °C (e). The specific capacitance against current density (f) (inset is the cyclic stability of FMCM-U electrode measured at 1 A g^{-1}).

137 F g^{-1} for FMCM at a current density of 0.5 A g^{-1}. The values are higher than those from previously synthesized carbon foams [37], and many mesoporous carbon electrode materials which were synthesized by a nanocasting method [38–40] or templated by the surfactant self-assembly [41]. As proved by the electrochemical impedance spectroscopy (Fig. 4e), the ESR of FMCM-U was comparable with FMCM. On the contrary, a much lower Warburg impedance of FMCM-U compared to FMCM (inset in Fig. 4e) further verified the short diffusion distance and fast ion diffusion speed in the mesoporous structure of FMCM-U[42,43]. At the low frequency region, the inclined lines for FMCM-U and FMCM are close to the theoretical vertical line and show characteristic features of pure capacitive behavior, indicating the electrolyte can easily access the pores [41,44]. When the current density was increased to 10 A g^{-1}, FMCM-U and FMCM accordingly exhibited a specific capacitance of 131 and 110 F g^{-1}, with high specific capacitance retention of 87% and 80% (Fig. 4f). The cyclic stability of the FMCM-U electrode was evaluated. As shown in inset of Fig. 4f, the FMCM-U material exhibits superior stability, and can recover its original performance after long-term storage. Such excellent performance of the supercapacitors is attributed to the intrinsic continuous mesporous carbon framework in the carbon skeleton that facilitates electron transport and avoids electron hopping among different particles in powders.

4. Conclusion

We have demonstrated a rapid and controllable synthesis of foam-like carbon monolith with uniform mesopores and macropores using an ultrasound-assisted air bubbling strategy. The carbon monoliths show uniform interconnected macropores and mesopores organized in a mesostructure manner located in the continuous carbon framework. This phenomenon suggests that the air bubbling together with ultrasound treatment can effectively induce self-assembly of the reactants. We believe that this approach can be applied to a much wider range of monomers and polymerization routes based on the features of different emulsions. More importantly, the current ultrasound-assisted air bubbling strategy is much easier and greener as compared to the conventional methods, in terms of time-saving, and being free of inorganic foaming agent and solid templates. Such foam-like carbon has potential applications in the fields of energy storage, adsorption and separation and catalysis.

Acknowledgments

We are grateful for the financial supports from National Science Fund for Distinguished Young Scholars (No. 21225312), Special Program for Basic Research of the Ministry of Science and Technology (No. 2012CB626802) and the Fundamental Research Funds for the Central Universities (No. DUT12ZD218).

REFERENCES

[1] Hu YS, Adelhelm P, Smarsly BM, Hore S, Antonietti M, Maier J. Synthesis of hierarchically porous carbon monoliths with highly ordered microstructure and their application in rechargeable lithium batteries with high-rate capability. Adv Funct Mater 2007;17(12):1873–8.
[2] Liang C, Li Z, Dai S. Mesoporous carbon materials: synthesis and modification. Angew Chem Int Ed 2008;47(20):3696–717.
[3] Gesser HD, Goswami PC. Aerogels and related porous materials. Chem Rev 1989;89(4):765–88.
[4] Li W-C, Lu A-H, Schüth F. Preparation of monolithic carbon aerogels and investigation of their pore interconnectivity by a nanocasting pathway. Chem Mater 2005;17(14):3620–6.
[5] Yuan ZY, Su BL. Insights into hierarchically meso-macroporous structured materials. J Mater Chem 2006;16(7):663–77.
[6] Xie K, Qin X, Wang X, Wang Y, Tao H, Wu Q, et al. Carbon nanocages as supercapacitor electrode materials. Adv Mater 2012;24(3):347–52.
[7] Wang DW, Li F, Liu M, Lu GQ, Cheng HM. 3D aperiodic hierarchical porous graphitic carbon material for high-rate electrochemical capacitive energy storage. Angew Chem Int Ed 2008;47(2):373–6.
[8] Raymundo-Piñero E, Kierzek K, Machnikowski J, Béguin F. Relationship between the nanoporous texture of activated carbons and their capacitance properties in different electrolytes. Carbon 2006;44(12):2498–507.
[9] Vix-Guterl C, Frackowiak E, Jurewicz K, Friebe M, Parmentier J, Beguin F. Electrochemical energy storage in ordered porous carbon materials. Carbon 2005;43(6):1293–302.
[10] Huang Y, Cai H, Feng D, Gu D, Deng Y, Tu B, et al. One-step hydrothermal synthesis of ordered mesostructured carbonaceous monoliths with hierarchical porosities. Chem Commun 2008;23:2641–3.
[11] Wang X, Bozhilov KN, Feng P. Facile preparation of hierarchically porous carbon monoliths with well-ordered mesostructures. Chem Mater 2006;18(26):6373–81.
[12] Adelhelm P, Hu YS, Chuenchom L, Antonietti M, Smarsly BM, Maier J. Generation of hierarchical meso- and macroporous carbon from mesophase pitch by spinodal decomposition using polymer templates. Adv Mater 2007;19(22):4012–7.
[13] Liu FJ, Li CJ, Ren LM, Meng XJ, Zhang H, Xiao FS. High-temperature synthesis of stable and ordered mesoporous polymer monoliths with low dielectric constants. J Mater Chem 2009;19(42):7921–8.
[14] Zhang FQ, Meng Y, Gu D, Yan Y, Yu CZ, Tu B, et al. A facile aqueous route to synthesize highly ordered mesoporous polymers and carbon frameworks with Ia(3)over-bard bicontinuous cubic structure. J Am Chem Soc 2005;127(39):13508–9.
[15] Kodama M, Yamashita J, Soneda Y, Hatori H, Kamegawa K. Preparation and electrochemical characteristics of N-enriched carbon foam. Carbon 2007;45(5):1105–7.
[16] Narasimman R, Prabhakaran K. Preparation of low density carbon foams by foaming molten sucrose using an aluminium nitrate blowing agent. Carbon 2012;50(5):1999–2009.
[17] Nishihara H, Kyotani T. Templated nanocarbons for energy storage. Adv Mater 2012;24(33):4473–98.
[18] Suslick KS, Fang M, Hyeon T. Sonochemical synthesis of iron colloids. J Am Chem Soc 1996;118(47):11960–1.
[19] Rana RK, Mastai Y, Gedanken A. Acoustic cavitation leading to the morphosynthesis of mesoporous silica vesicles. Adv Mater 2002;14(19):1414–8.
[20] Binks BP, Duncumb B, Murakami R. Effect of pH and salt concentration on the phase inversion of particle-stabilized foams. Langmuir 2007;23(18):9143–6.
[21] Kim Y, Jo C, Lee J, Lee CW, Yoon S. An ordered nanocomposite of organic radical polymer and mesocellular carbon foam as cathode material in lithium ion batteries. J Mater Chem 2012;22(4):1453–8.
[22] Oda Y, Fukuyama K, Nishikawa K, Namba S, Yoshitake H, Tatsumi T. Mesocellular foam carbons: aggregates of hollow carbon spheres with open and closed wall structures. Chem Mater 2004;16(20):3860–6.
[23] Kim TY, Lee HW, Stoller M, Dreyer DR, Bielawski CW, Ruoff RS, et al. High-performance supercapacitors based on poly(ionic liquid)-modified graphene electrodes. ACS Nano 2011;5(1):436–42.
[24] Hao GP, Li WC, Qian D, Wang GH, Zhang WP, Zhang T, et al. Structurally designed synthesis of mechanically stable poly(benzoxazine-co-resol)-based porous carbon monoliths and their application as high-performance CO_2 capture sorbents. J Am Chem Soc 2011;133(29):11378–88.
[25] Li X, Basso MC, Braghiroli FL, Fierro V, Pizzi A, Celzard A. Tailoring the structure of cellular vitreous carbon foams. Carbon 2012;50(5):2026–36.
[26] Narasimman R, Prabhakaran K. Preparation of carbon foams by thermo-foaming of activated carbon powder dispersions in an aqueous sucrose resin. Carbon 2012;50(15):5583–93.
[27] Liu MX, Gan LH, Zhao FQ, Xu HX, Fan XZ, Tian C, et al. Carbon foams prepared by an oil-in-water emulsion method. Carbon 2007;45(13):2710–2.
[28] Skrabalak SE. Ultrasound-assisted synthesis of carbon materials. Phys Chem Chem Phys 2009;11(25):4930–42.
[29] Jun S, Joo SH, Ryoo R, Kruk M, Jaroniec M, Liu Z, et al. Synthesis of new, nanoporous carbon with hexagonally ordered mesostructure. J Am Chem Soc 2000;122(43):10712–3.
[30] Zhao D, Feng J, Huo Q, Melosh N, Fredrickson GH, Chmelka BF, et al. Triblock copolymer syntheses of mesoporous silica with periodic 50 to 300 angstrom pores. Science 1998;279(5350):548–52.
[31] Yang XX, Liu L, Wu MH, Wang WL, Bai XD, Wang EG. Wet-chemistry-assisted nanotube-substitution reaction for high-efficiency and bulk-quantity synthesis of boron- and nitrogen-codoped single-walled carbon nanotubes. J Am Chem Soc 2011;133(34):13216–9.
[32] Su F, Poh CK, Chen JS, Xu G, Wang D, Li Q, et al. Nitrogen-containing microporous carbon nanospheres with improved capacitive properties. Energy Environ Sci 2011;4(3):717–24.
[33] Arrigo R, Haevecker M, Wrabetz S, Blume R, Lerch M, McGregor J, et al. Tuning the acid/base properties of nanocarbons by functionalization via amination. J Am Chem Soc 2010;132(28):9616–30.
[34] Brinker CJ, Lu Y, Sellinger A, Fan H. Evaporation-induced self-assembly: nanostructures made easy. Adv Mater 1999;11(7):579–85.
[35] Liang CD, Hong KL, Guiochon GA, Mays JW, Dai S. Synthesis of a large-scale highly ordered porous carbon film by self-assembly of block copolymers. Angew Chem Int Ed 2004;43(43):5785–9.
[36] Meng Y, Gu D, Zhang FQ, Shi YF, Cheng L, Feng D, et al. A family of highly ordered mesoporous polymer resin and

carbon structures from organic-organic self-assembly. Chem Mater 2006;18(18):4447–64.
[37] Moglie F, Micheli D, Laurenzi S, Marchetti M, Mariani Primiani V. Electromagnetic shielding performance of carbon foams. Carbon 2012;50(5):1972–80.
[38] Liu HJ, Jin LH, He P, Wang CX, Xia YY. Direct synthesis of mesoporous carbon nanowires in nanotubes using MnO2 nanotubes as a template and their application in supercapacitors. Chem Commun 2009(44):6813–5.
[39] Liu HJ, Cui WJ, Jin LH, Wang CX, Xia YY. Preparation of three-dimensional ordered mesoporous carbon sphere arrays by a two-step templating route and their application for supercapacitors. J Mater Chem 2009;19(22):3661–7.
[40] Li HQ, Luo JY, Zhou XF, Yu CZ, Xia YY. An ordered mesoporous carbon with short pore length and its electrochemical performances in supercapacitor applications. J Electrochem Soc 2007;154(8):A731–6.
[41] Li W, Zhang F, Dou YQ, Wu ZX, Liu HJ, Qian XF, et al. A self-template strategy for the synthesis of mesoporous carbon nanofibers as advanced supercapacitor electrodes. Adv Energy Mater 2011;1(3):382–6.
[42] Huang CH, Zhang Q, Chou TC, Chen CM, Su DS, Doong RA. Three-dimensional hierarchically ordered porous carbons with partially graphitic nanostructures for electrochemical capacitive energy storage. ChemSusChem 2012;5(3):563–71.
[43] Huang CW, Hsu CH, Kuo PL, Hsieh CT, Teng HS. Mesoporous carbon spheres grafted with carbon nanofibers for high-rate electric double layer capacitors. Carbon 2011;49(3):895–903.
[44] Zhang Y, Liu C, Wen B, Song X, Li T. Preparation and electrochemical properties of nitrogen-doped multi-walled carbon nanotubes. Mater Lett 2011;65(1):49–52.